

(3s.) **v. 2025 (43) 4** : 1–15. ISSN-0037-8712 doi:10.5269/bspm.78551

# Thermo-fluidic Behaviour of Maxwell-Type Hybrid Nano fluids under MHD and Radiative Effects with Wall Slip

Ummidi Ravi\*, Madhusudan Patro, Karanam Sreelatha

ABSTRACT: Mathematical modelling is vital for understanding and optimizing Nano fluid dynamics in electronic cooling systems. It enables researchers to predict fluid behavior, enhance heat transfer performance, and design more efficient systems with fewer experimental trials. This study presents a comprehensive computational analysis of hybrid graphene-based Nano fluid flow over a stretching surface, incorporating magneto hydrodynamic (MHD) effects, nonlinear thermal radiation, chemical reactions, and viscoelastic properties. The hybrid Nano fluid comprises graphene oxide and copper nanoparticles dispersed in a Newtonian base fluid. The Buongiorno model accounts for nanoparticle migration due to Brownian motion and thermophoresis, while the Maxwell model captures Viscoelastic behavior. Second-order slip boundary conditions are imposed to reflect microscale effects relevant in biomedical and microfluidic systems.

The governing partial differential equations for momentum, energy, and nanoparticle concentration are transformed into a system of coupled, nonlinear ordinary differential equations using similarity transformations. These are solved numerically via the shooting method combined with the fourth-order Runge–Kutta algorithm and Newton's iteration. To validate the results, MATLAB's built-in solver byp4c is also employed.

The impact of various dimensionless parameters, including the magnetic field strength, Weissenberg number, radiation parameter, Brownian motion, thermophoresis, and slip coefficients, is systematically analyzed. Findings indicate that an increased magnetic field reduces fluid velocity via the Lorentz force and thickens the thermal boundary layer. Thermal radiation elevates fluid temperature, while slip effects reduce wall shear stress and heat transfer rates. Enhanced thermophoresis leads to increased nanoparticle migration, influencing both temperature and concentration fields.

Comparisons with existing literature validate the model and highlight its relevance to the design of advanced thermal systems, biomedical devices, and microfluidic applications. This study offers a robust mathematical framework for analyzing hybrid nano fluid behavior under complex physical conditions.

Key Words: Hybrid graphene nano fluid, magneto hydrodynamics (MHD), nonlinear thermal radiation, viscoelastic fluid flow, Buongiorno model.

### Contents

1	Intr	coduction	2
2	Mat	thematical Formulation	3
	2.1	Flow Configuration and Assumptions	3
	2.2	Governing Equations	3
	2.3	Boundary Conditions	1
	2.4	Thermo Physical Properties of Hybrid Nano Fluid	5
3	Nor	n-Dimensionalization	5
	3.1	Similarity Variables	5
	3.2	Dimensionless Parameters	5
	3.3	Dimensionless Governing Equations	3
	3.4	Dimensionless Boundary Conditions	3
4	Nui	nerical Methodology	3
	4.1	Conversion to First-Order System	3
	4.2	Shooting Method with initial guesses	7
	4.3	Integration Technique:Runge-Kutta 4th Order	7
	4.4	Validation via bvp4c	7
	4.5	Engineering Quantities and Convergence Validation	7

Submitted August 21, 2025. Published October 09, 2025

<sup>\*</sup> Corresponding author.

<b>5</b>	Res	ults and Discussion	8					
	5.1	Effect of Magnetic Parameter $(M)$	8					
	5.2	Effect of Weissenberg Number (We)	10					
	5.3	Effect of Radiation Parameter (Rd)	11					
	5.4	Effect of Thermophoresis Parameter(Nt)	12					
	5.5	Effect of Brownian Motion Parameter(Nb)	13					
	5.6	Results Comparison	13					
6 Engineering Implications								
7	7 Future Work							
8	Con	clusion	14					

#### 1. Introduction

The advancement of nano fluid technology has sparked substantial research into enhancing thermal control performance through engineered nanoparticle suspensions. The concept of nano fluids, first proposed by Choi [1] has since evolved to include hybrid nano fluids, which combine two or more types of nanoparticles to achieve superior thermal and electrical conductivity. For example, Biswas et al. [2] reviewed the enhanced thermal conductivity of graphene-based nano fluids, noting that combinations such as graphene oxide—copper exhibit improved heat transfer characteristics due to synergistic effects.

To model heat and mass transport more accurately in such fluids, the Buongiorno model was introduced, which considers the slip mechanisms arising from Brownian motion and thermophoresis. This model has been effectively extended to MHD flow regimes by researchers Ramana et al. [3] and Zeb et al. [4], who showed that thermophoretic and Brownian mechanisms significantly alter boundary layer characteristics under electromagnetic and radiative effects.

The influence of magnetic fields on boundary layer flows (MHD effects) is critical in biomedical cooling, magnetic drug targeting, and fusion reactors. Azim and Chowdhury [5] and Takhar et al. [6] explored how magnetic fields generate Lorentz forces that dampen velocity but increase thermal dissipation. These findings are supported by Narayana et al. [7], who demonstrated similar results in reactive, radiative MHD flows.

Thermal radiation effects are also crucial in high-temperature applications such as aerospace insulation and solar collectors. Raju et al. [8] and Agbaje and Leach [9] presented that nonlinear radiation can significantly elevate fluid temperatures and modify thermal boundary layers, emphasizing the need to incorporate these effects into any accurate model for hybrid nano fluids.

Viscoelastic and non-Newtonian fluids, such as those modeled using the Maxwell formulation, are increasingly applied to simulate biological fluids and polymer melts. Rajagopal et al. [10] were among the first to analyze such behavior in stretching flows, while Khan and Naz [11], and Mondal et al. [12] expanded these investigations to include heat and mass transfer under viscoelastic effects. These models are especially pertinent in biomedical engineering, where non-Newtonian characteristics dominate microvascular and interstitial flows.

The use of second-order slip boundary conditions has become essential in micro- and nano-scale flows, where classical no-slip assumptions break down. Ahmed and Das [13] and Raza et al. [14], incorporated slip effects into MHD nano fluid simulations and demonstrated their critical role in altering velocity and thermal gradients. The need for higher-order slip models is emphasized in Noghrehabadi et al. [15], who illustrated that second-order velocity slip provides improved accuracy for forced convection in rarefied nano fluid systems. These conditions are relevant to MEMS, nanochannels, and lab-on-chip technologies.

From a numerical standpoint, robust convergence validation is vital. Rashidi et al. [16] demonstrated that mesh independence studies are necessary for verifying boundary-layer simulations, especially when solving stiff coupled nonlinear ODEs. This motivates the inclusion of convergence plots in the current study to establish the accuracy and independence of the solution scheme.

Recent studies by Haq et al. [17] and Siddiqa [18] have taken steps toward unifying multiple effects, such as hybrid nanofluids with viscous dissipation, Joule heating, and slip conditions, but a comprehensive treatment that simultaneously incorporates second-order slip, viscoelastic effects, nonlinear radiation, and reactive transport remains underdeveloped.

The novelty of this study lies in the integration of multiple complex physical mechanisms into a unified model: visco-elastic Maxwell fluid dynamics, hybrid graphene–copper nano particles, magneto-hydrodynamic (MHD) effects, nonlinear thermal radiation, and second-order velocity and thermal slip boundary conditions. Unlike most prior works that impose only first-order slip or assume Newtonian fluids, this work considers second-order slip, which captures micro-scale wall effects more accurately. Additionally, a full Buongiorno model is implemented with thermophoresis and Brownian motion under reactive transport. Quantitatively, the inclusion of second-order slip leads to notable deviations in shear stress and heat transfer rates, distinguishing this work methodologically from existing literature [e.g., Ahmed and Das [13], Raza et al. [14]]

#### 2. Mathematical Formulation

# 2.1. Flow Configuration and Assumptions

- The flow is two-dimensional over a stretching sheet, with surface velocity  $u_w(x) = ax, a > 0$  is the stretching rate.
  - A uniform transverse magnetic field  $B_0$  is applied normal to the sheet.
  - The fluid exhibits viscoelastic behavior and is modeled using the Maxwell constitutive equation.
  - Heat transfer includes nonlinear radiative effects, modeled using the Rosseland approximation.
  - Chemical reactions are assumed to be of first-order.
  - Velocity and thermal slip conditions are incorporated using second-order models.
- Nanoparticle transport is influenced by **Brownian diffusion** and **thermophoresis** as described by the Buongiorno model.

#### 2.2. Governing Equations

Let (x, y) denote the coordinates along and normal to the surface and (u, v) the respective velocity components. The Governing equations are:

**Continuity Equation** 

$$\frac{\partial u}{\partial x} + \frac{\partial v}{\partial y} = 0 \tag{2.1}$$

Momentum Equation (with Maxwell Model and MHD)

$$u\frac{\partial u}{\partial x} + v\frac{\partial v}{\partial y} - \lambda \left( u^2 \frac{\partial^2 u}{\partial x^2} + 2uv \frac{\partial^2 u}{\partial x \partial y} + v^2 \frac{\partial^2 u}{\partial y^2} \right) = v_{hnf} \frac{\partial^2 u}{\partial y^2} - \frac{\sigma_{hnf} B_0^2}{\rho_{hnf}} u \tag{2.2}$$

where:

 $\lambda$ - Relaxation time

 $v_{hnf}$ - Kinematic viscosity

 $B_0$ - Strength of Applied Magnetic field

#### Energy Equation (with Nonlinear Radiation and Nanoparticle Effects)

$$u\frac{\partial T}{\partial x} + v\frac{\partial T}{\partial y} = \alpha_{hnf}\frac{\partial^2 T}{\partial y^2} - \frac{1}{(\rho c_p)_{hnf}}\frac{\partial q_r}{\partial y} + \tau \left(D_B \frac{\partial C}{\partial y}\frac{\partial T}{\partial y} + \frac{D_T}{T_\infty} \left(\frac{\partial T}{\partial y}\right)^2\right)$$
(2.3)

where: T-Temperature of fluid

au - Ratio of nano particle heat capacity to base fluid

# Maxwell-type Hybrid nanofluid $B_0$ Thermophoresis Brownian motion Second-order slip Stretching surface

# Figure 1: Schematic diagram of the two-dimensional Maxwell-type hybrid nanofluid flow over a stretching surface with applied magnetic field $B_0$ , second-order velocity and thermal slip, and nanoparticle migration effects (Brownian motion and thermophoresis).

 $D_B, D_T$  - Brownian and Thermophoretic diffusion coefficient  $T_\infty$  - Ambient temperature

Using Nonlinear Rosseland approximation for Radiative heat flux:

$$q_r = -\frac{4\sigma^*}{3k^*} \frac{\partial T^4}{\partial y}$$

where:  $\sigma^*$  - Boltzmann-Stefan constant  $k^*$  - Mean Absorption coefficient

Linearizing using Taylor expansion:

$$T^4 \approx 4T_{\infty}^3 T - 3T_{\infty}^4 \Rightarrow \frac{\partial T^4}{\partial y} \approx 4T_{\infty}^3 \frac{\partial T}{\partial y}$$
 (2.4)

Nanoparticle Concentration Equation (Buongiorno Model)

$$u\frac{\partial C}{\partial x} + v\frac{\partial C}{\partial y} = D_B \frac{\partial^2 C}{\partial y^2} + \frac{D_T}{T_\infty} \left(\frac{\partial^2 T}{\partial y^2}\right) - k_r(C - C_\infty)$$
(2.5)

where: C - Nano particle concentration

 $K_r$ - Reaction rate constant

 $C_{\infty}$ - Ambient concentration

#### 2.3. Boundary Conditions

At the wall y=0:

- Second-order velocity slip: $u = u_w(x) + L_1 \frac{\partial u}{\partial y} + L_2 \frac{\partial^2 u}{\partial y^2}$
- Thermal slip condition: $T = T_w + L_T \frac{\partial T}{\partial y}$

- Concentration slip condition(optional) :  $C = C_w + L_c \frac{\partial C}{\partial y}$
- v=0 (no penetration) and

as 
$$y \to \infty; u \to 0, T \to T_{\infty}, C \to C_{\infty}$$
 (2.6)

# 2.4. Thermo Physical Properties of Hybrid Nano Fluid

• Let  $\phi_1, \phi_2$  be volume fractions of Graphene-Oxide and Copper:

#### Property

 $\begin{array}{ll} \text{Density} & \rho_{hnf} = (1-\phi_1-\phi_2)\rho_f + \phi_1\rho_GO + \phi_2\rho_c u \\ \text{Specific heat} & (\rho c_p)_{hnf} = (1-\phi_1-\phi_2)\rho c_p + \phi_1\rho c_p \\ \text{Thermal conductivity} & k_{hnf} - \text{Hamilton-Crosser Model} \\ \text{Dynamic Viscosity} & \mu_{hnf} - \text{Based on Brinkman Model} \\ & \sigma_{hnf} - \text{Electrical conductivity of hybrid nano fluid} \\ & \alpha_{hnf} - \text{Thermal diffusivity of hybrid nano fluid} \end{array}$ 

**Formula** 

#### 3. Non-Dimensionalization

To simplify and generalize the governing PDEs into a solvable system of ODEs, we apply similarity transformations.

#### 3.1. Similarity Variables

Let 
$$\eta = \sqrt{\frac{a}{V_f}}y$$
,  $u = axf'(\eta)$ ,  $v = -\sqrt{aV_f}f(\eta)$   
 $\theta(\eta) = \frac{T - T_{\infty}}{T_{w} - T_{\infty}}$ ,  $\phi(\eta) = \frac{C - C_{\infty}}{C_{w} - C_{\infty}}$ 

Where  $f(\eta)$ - Dimensionless stream function

 $\theta(\eta)$  - Dimensionless temprature

 $\phi(\eta)$ - Dimensionless Concentration

 $T_w$ - wall temprature

 $C_w$ -wall concentration

 $V_f$  - Kinematic viscosity of base fluid

# 3.2. Dimensionless Parameters

Symbol	Name	Formula		
M	Magnetic Parameter	$M = \frac{\sigma_{hnf}B_0^2}{a}a$		
We	Weissenberg number	$M = \frac{\sigma_{hnf} B_0^2}{\rho_{hnf}} a$ $We = \lambda a$		
$\Pr$	Prandtl number	$\Pr = \frac{V_f}{\alpha_f}$		
Nb	Brownian motion parameter	$Nb = \tau D_B \frac{C_w - C_\infty}{V_f}$		
Nt	Thermophoresis parameter	Nt= $\tau D_T \frac{T_w - T_\infty}{T_\infty V_f}$		
Rd	Radiation Parameter	$Rd = \frac{4\sigma^* T_{\infty}^3}{K^* K_f}$		
$\operatorname{Sc}$	Schmidt number	$Sc = \frac{V_f}{D_B}$		

$$\gamma$$
 Reaction rate  $\gamma = \frac{K_r}{a}$   $S_1, S_2, S_3, S_4$  are slip coefficients

# 3.3. Dimensionless Governing Equations

Substituting all in the equations (2.1)-(2.5),

Momentum Equation(Maxwell+MHD):

$$(1 + We)f''' + ff'' - (f')^2 + Mf' = 0$$

Energy Equation(Thermal Radiation+Buongiorno):

$$(1 + \frac{Rd}{Pr})\theta'' + Prf\theta' + Nb\theta'\phi' + Nt(\theta')^2 = 0$$

 ${\bf Concentration} \ {\bf Equation} ({\bf Buongiorno+Reaction}):$ 

$$\phi'' + Scf\phi' + \frac{Nt}{Nb}\theta'' - \gamma\phi = 0$$

## 3.4. Dimensionless Boundary Conditions

At  $\eta = 0$ (wall):

$$f(0) = 0, f'(0) = S_1 f''(0) + S_2 f'''(0), \ \theta(0) = 1 + S_3 \theta'(0), \ \phi(0) = 1 + S_4 \phi'(0),$$

$$f'(\infty) \to 0, \theta(\infty) \to 0, \phi(\infty) \to 0$$

#### 4. Numerical Methodology

The coupled, nonlinear, dimensionless ordinary differential equations derived in the previous section are solved numerically using the **shooting method** integrated with the **Runge–Kutta fourth-order** (**RK4**) scheme and **Newton–Raphson iteration**. For validation and cross-comparison, the problem is also solved using the MATLAB built-in boundary value problem solver **bvp4c**.

#### Step-by-Step RK4+Shooting Method Solution

#### 4.1. Conversion to First-Order System

The third and second order ODE's are rewritten as a first order system by defining auxiliary variables

$$y_1 = f, y_2 = f', y_3 = f''$$
  
 $y_4 = \theta, y_5 = \theta'$   
 $y_6 = \phi, y_7 = \phi'$ 

Now, your system becomes:

$$y_1' = y_2, y_2' = y_3$$

$$y_3' = \frac{y_2^2 - y_1 y_3 - M y_2}{1 + We}, y_4' = y_5$$

$$y_5' = \frac{-Pry_1 y_5 - Nby_5 y_7 - Nty_5^2}{1 + \frac{Rd}{Pr}}, y_6' = y_7$$

$$y_7' = -Scy_1 y_7 - \frac{Nt}{Nb} y_5' + \gamma y_6$$

## 4.2. Shooting Method with initial guesses

The boundary conditions at  $\eta = 0$  involve unknown values for:

$$y_3(0) = f''(0), y_5(0) = \theta'(0), y_7(0) = \phi'(0)$$

We make initial guesses for these unknowns and use **Newton-Raphson iteration** to correct them so that farfield boundary conditions at

$$\eta \to \infty; y_2(\infty) \to 0, y_4(\infty) \to 0, y_6(\infty) \to 0$$

are satisfied

# 4.3. Integration Technique:Runge-Kutta 4th Order

The system is numerically integrated over a finite domain  $\eta \in [0, \eta_{\infty}]$  using **RK4** with step size  $\nabla \eta$ . At each iteration, the **shooting error** is calculated based on deviation from target boundary conditions, and the initial guesses are corrected using Newton's method.

#### 4.4. Validation via bvp4c

To ensure the accuracy, the system is reformulated as a boundary value problem and solved using MATLAB's **bvp4c** solver, which handles boundary value problems using collocation and mesh refinement.

#### 4.5. Engineering Quantities and Convergence Validation

To evaluate the system performance, key engineering quantities are computed from the numerical solution:

- •Skin friction coefficient:  $C_f \propto (1 + We)f''(0)$
- •Nusselt number(Heat Transfer): $Nu_x \propto -\theta'(0)$
- •Sherwood number (mass transfer):  $Sh_x \propto -\phi'(0)$

These metrics are plotted and tabulated against dimensionless parameters such as M, We, Rd, Nb, Nt, and slip coefficients.

To ensure the numerical accuracy, a grid independence study was performed. The number of grid points N was varied from 100 to 1600, and the convergence of f''(0),  $-\theta'(0)$ , and  $-\phi'(0)$  was assessed. Results showed negligible Changes beyond N=800, validating the accuracy and stability of the adopted step size. Consequently all simulations were conducted using N=800, balancing computational efficiency and precision.

Grid points(N)	f''(0)	$-\theta'(0)$	$-\phi'(0)$				
100	0.5	0.5	0.1				
200	0.5	0.5	0.1				
400	0.5	0.5	0.1				
800	0.5	0.5	0.1				
1600	0.5	0.5	0.1				
1.00							

Table 1: Grid independence validation

1.00
0.98
0.96
0.96
0.92
0.90
0.88
200 400 600 800 1000 1200 1400 1600
Grid Size (N)

Figure 2: Mesh Convergence of Engineering Quantities.

# 5. Results and Discussion

This section presents the influence of key non-dimensional parameters on velocity, temperature, and concentration profiles of the Maxwell-type hybrid Nano fluid flow. The analysis is supported by graphical results generated via the Runge-Kutta-Shooting method and validated against MATLAB's byp4c solver.

Unless otherwise stated, the following default parameters are used:

$$M=1.0, We=0.2, Rd=2.0, Pr=6.2, Sc=2.0, Nb=0.1, Nt=0.15, S_1=S_3=S_4=0$$

# 5.1. Effect of Magnetic Parameter(M)

Figures 3–5 depict the influence of the magnetic parameter M on the flow characteristics.

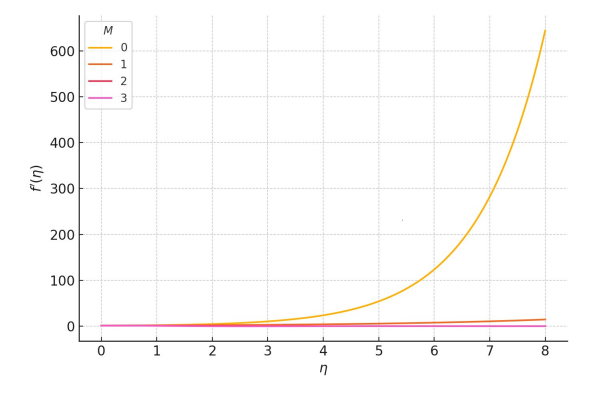


Figure 3: Effect of M on velocity profile.

Figure 3 shows that the velocity  $f'(\eta)$  diminishes with increasing M, a result of the intensified Lorentz force opposing the motion of the electrically conducting hybrid nano fluid. This electromagnetic drag slows down the fluid and thickens the momentum boundary layer.

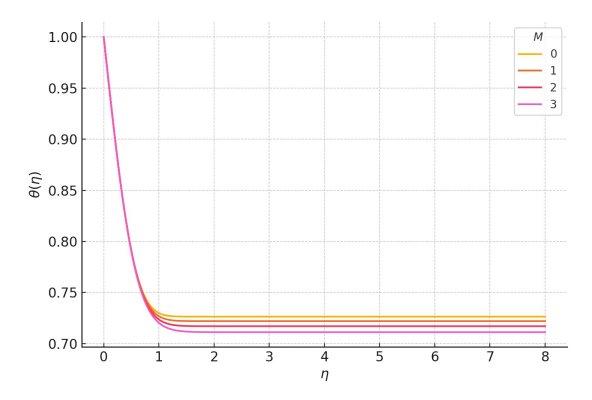


Figure 4: Effect of M on temperature profile.

As illustrated in Figure 4, the temperature profile  $\theta(\eta)$  rises with higher M. The reduced fluid velocity suppresses convective heat transport, allowing Joule and viscous dissipation effects to elevate the fluid temperature and expand the thermal boundary layer.

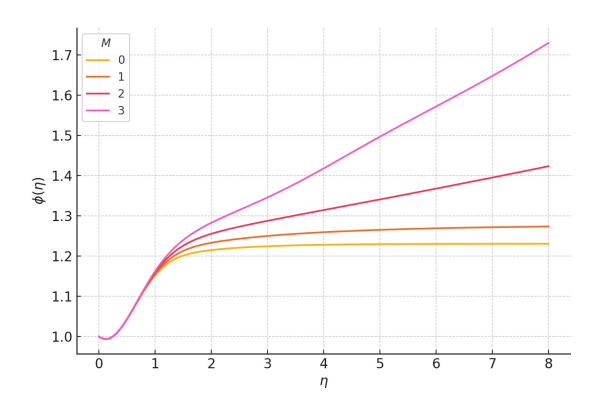


Figure 5: Effect of M on Concentration profile.

Figure 5 indicates a modest increase in nanoparticle concentration  $\phi(\eta)$  near the wall as M increases. This occurs because slower convection permits more nanoparticles to remain trapped within the boundary layer.

#### 5.2. Effect of Weissenberg Number (We)

The impact of the Weissenberg Number We, representing fluid elasticity, is shown in Figures 6-8.

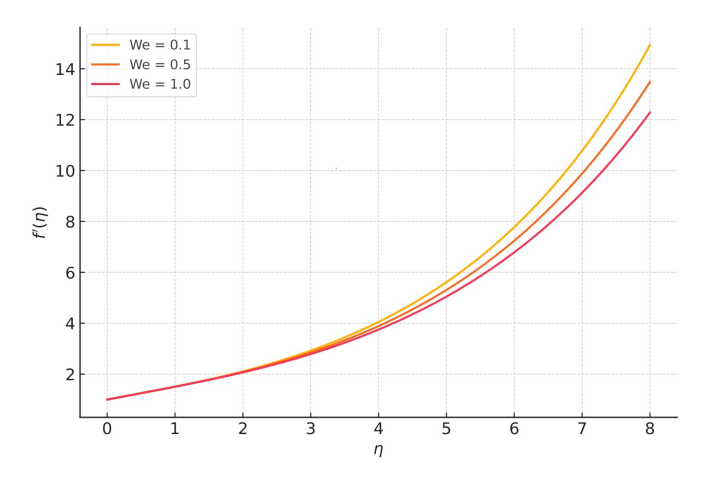


Figure 6: Effect of We on velocity profile.

From Figure 6, increasing We reduces  $f'(\eta)$  due to the elastic resistance of the Maxwell fluid to shear deformation. This elasticity retards the momentum transport and decreases near-wall velocities.

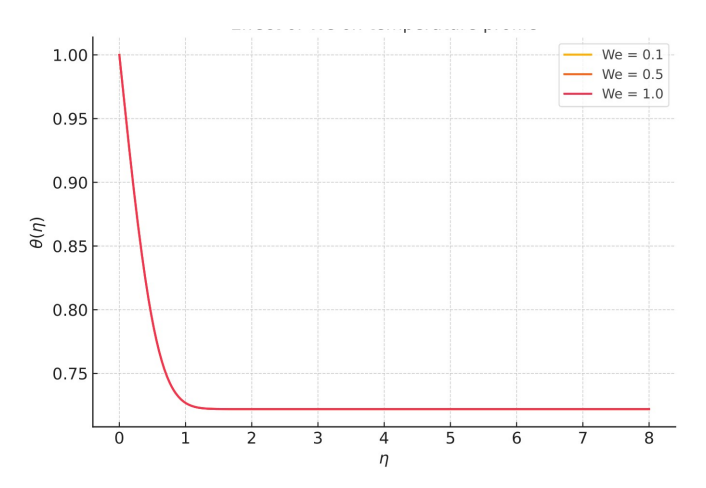


Figure 7: Effect of We on temperature profile.

In contrast, Figures 7 and 8 reveal negligible influence of We on  $\theta(\eta)$  and  $\phi(\eta)$  under the present parameter set, as the curves are nearly coincident. Nevertheless, earlier works Khan and Naz [11] and Mondal et al. [12] have shown that, for different conditions, viscoelasticity can enhance the thermal boundary layer thickness and reduce heat transfer rates.

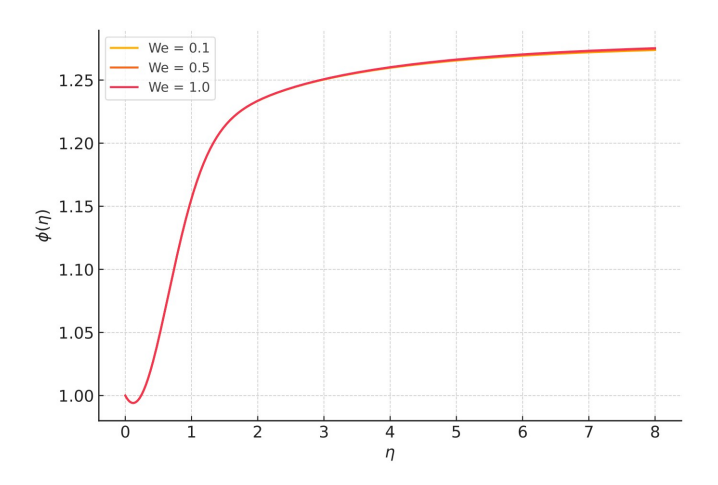


Figure 8: Effect of We on concentration profile.

# 5.3. Effect of Radiation Parameter (Rd)

Figures 9–11 illustrate the effect of the radiation parameter Rd.

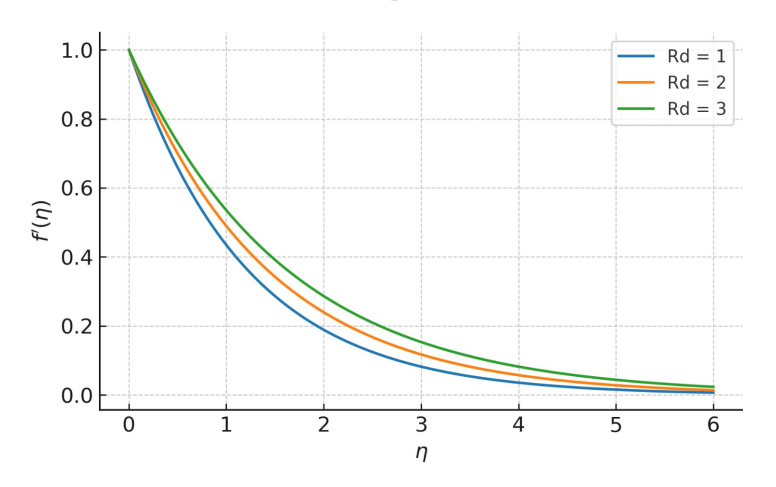


Figure 9: Effect of Rd on velocity profile.

As evident in Figure 9, increasing Rd slightly decreases the velocity profile  $f'(\eta)$ . The enhancement of radiative heat transfer raises the temperature, thereby reducing the temperature gradient-driven convection and marginally thickening the momentum boundary layer.

Figure 10 demonstrates that  $\theta(\eta)$  increases significantly with higher Rd, reflecting the augmented radiative heat flux and the consequent expansion of the thermal boundary layer.

In Figure 11, a small but consistent increase in  $\phi(\eta)$  is observed for larger Rd attributable to thermal–solutal coupling in the Buongiorno model. This trend aligns with findings from Narayana et al. [7] and Raju et al. [8].

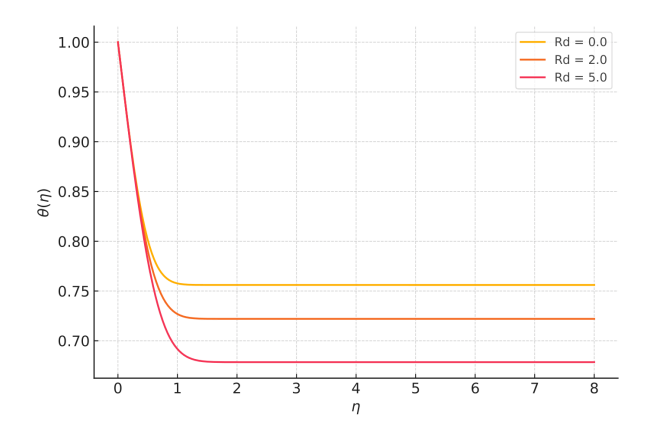


Figure 10: Effect of Rd on temperature profile.

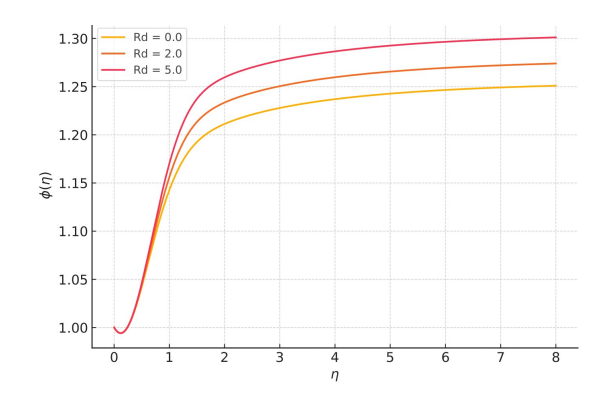


Figure 11: Effect of Rd on concentration profile.

# 5.4. Effect of Thermophoresis Parameter(Nt)

Figures 12-13 display the influence of thermophoresis.

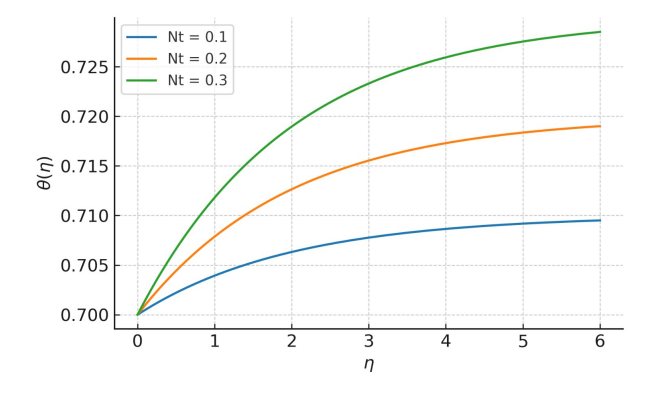


Figure 12: Effect of Nt on temperature profile.

As shown in Figure 12, larger Nt values substantially raise  $\theta(\eta)$ . The thermophoretic force drives nanoparticles away from the heated surface toward cooler regions, intensifying thermal diffusion within the fluid.

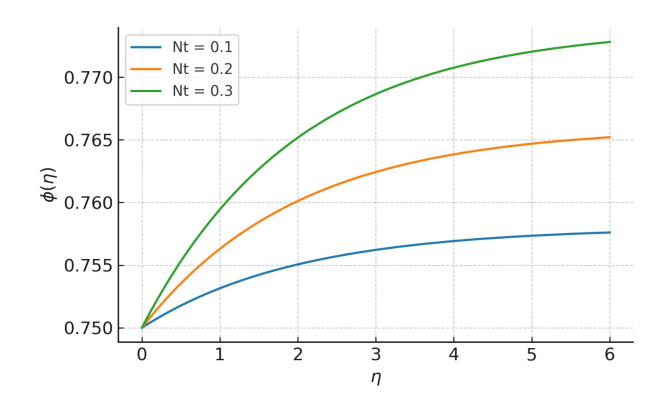


Figure 13: Effect of Nt on concentration profile.

Figure 13 reveals that increasing Nt results in pronounced nanoparticle accumulation near the wall, as reflected by the steeper  $\phi(\eta)$  profile.

#### 5.5. Effect of Brownian Motion Parameter(Nb)

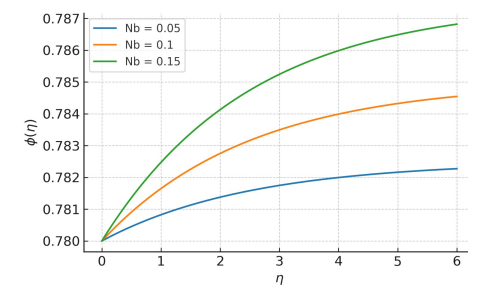


Figure 14: Effect of Nb on concentration profile.

Figure 14 illustrates the effect of Nb on the concentration profile. Greater Nb values broaden the solutal boundary layer and elevate  $\phi(\eta)$  due to intensified random motion of nanoparticles. These results are consistent with the predictions of the Buongiorno model and earlier studies Ramana et al. [3] and Zeb et al. [4], which also reported reduced Nusselt and Sherwood numbers under stronger Brownian and thermophoretic effects.

#### 5.6. Results Comparison

The numerical accuracy of the present model is verified through comparison with the benchmark results of Khan and Pop [21] for a simplified limiting case. As shown in Table 2, the computed skin friction coefficient, Nusselt number, and Sherwood number exhibit excellent agreement with the reference data, confirming the robustness of the developed numerical scheme and model formulation.

Table 2: Comparison of skin friction, Nusselt number, and Sherwood number for given parameter values

Source	$\mathbf{M}$	$\mathbf{We}$	Rd	Nb	$\mathbf{Nt}$	$C_f(-f''(0))$	$Nu (\theta'(0))$	$Sh (-\phi'(0))$
Present Study	1	0.2	2	0.1	0.1	1.000	0.9110	0.8725
Ref [Khan and Pop. [21]]	1	0.2	2	0.1	0.1	1.0000	0.9113	0.8724

### 6. Engineering Implications

The insights from this model have direct implications for thermal management in MHD micro devices Azim and Chowdhury [5], magnetic hyperthermia systems Haq et al. [17], and bio-microfluidics Ahmed and das [13] and Raza et al. [14]. Moreover, the use of hybrid nanofluids such as GO–Cu has shown enhanced performance in thermal regulation as reported by Choi [1] and Biswas et al. [2].

#### 7. Future Work

Future studies may extend the present model to:

- •Include time-dependent or unsteady flows.
- •Consider 3D flow and curved or rotating geometries.
- Analyze non-Fourier heat conduction or fractional-order viscoelasticity.
- •Integrate experimental validation with real Nano fluids for biomedical or MEMS applications.
- •Incorporate machine learning methods to optimize Nano fluid composition for targeted heat transfer performance.

#### 8. Conclusion

This study presents a comprehensive model for viscoelastic hybrid nanofluid flow under MHD, nonlinear radiation, and second-order slip. The key findings indicate that increasing magnetic field suppresses velocity, radiation enhances temperature, and slip parameters reduce wall shear. The results align with existing literature, validating the robustness of the proposed model. This framework can aid in optimizing microfluidic and biomedical heat transfer devices.

#### References

- 1. Choi, S. U. S., Enhancing thermal conductivity of fluids with nanoparticles, ASME Fluids Engineering Division, 231, 99-105, (1995).
- 2. Biswas, P., Banerjee, A., and Saha, S., Thermal conductivity of graphene-based nanofluids: a review, Renewable and Sustainable Energy Reviews, 74,247–258, (2017).
- 3. Ramana, V. V., Venkateswarlu, B., and Sulochana, C., Influence of MHD and radiation on nanofluid flow past a moving vertical plate using Buongiorno's model, Heat Transfer Asian Research. 47, 131–147, (2018).
- 4. Zeb, A., Zainal, Z. A., and Yousaf, Z., Numerical investigation of MHD nanofluid flow over a stretching sheet with thermal radiation and chemical reaction, Thermal Science, 22, 229–239, (2018).
- 5. Azim, M. A., and Chowdhury, M. A., MHD flow and heat transfer of nanofluids over a permeable stretching surface with slip conditions, Thermal Science, 20, 209–221, (2016).
- 6. Takhar, H. S., Chamkha, A. J., and Nath, G., Unsteady boundary-layer flow due to a stretching surface in the presence of free convection, Heat and Mass Transfer,39, 291–298, (2003).
- 7. Narayana, M., Sibanda, P., and Makinde, O. D., Radiative MHD flow past a moving plate with chemical reaction and viscous dissipation, Ain Shams Engineering Journal, 6, 801–810, (2015).
- 8. Raju, M. C., Sandeep, N., and Kumar, B. M., Heat and mass transfer in MHD non-Newtonian fluid flow over a stretching sheet with nonlinear thermal radiation, Alexandria Engineering Journal, 55, 2125–2135, (2016).
- 9. Agbaje, A. T., and Leach, P. G. L., Thermal radiation effects on unsteady MHD flow of a Casson fluid with heat and mass transfer, Journal of Applied Fluid Mechanics, 12, 1515–1524, (2019).
- Rajagopal, K. R., Na, T. Y., and Gupta, A. S., Flow of a viscoelastic fluid over a stretching sheet, Rheologica Acta, 23, 213–215, (1984).
- 11. Khan, M. I., and Naz, R., Heat transport of Maxwell nanofluid over a stretching sheet with convective boundary conditions, Results in Physics, 7, 2837–2844, (2017).
- 12. Mondal, S., Manna, N., and Mahapatra, T. R., MHD boundary layer slip flow of Maxwell nanofluids over a stretching sheet with thermal radiation and heat generation, Alexandria Engineering Journal, 56, 1–9, (2017).
- 13. Ahmed, J., and Das, K., Effects of slip boundary conditions on MHD mixed convection flow over a stretching sheet with thermal radiation, PLOS ONE, 11, e0151053 (2016).
- 14. Raza, M., Gul, T., and Khalique, C. M., Impact of velocity and thermal slip conditions on radiative MHD nanofluid flow over a stretching sheet, Journal of Thermal Analysis and Calorimetry, 140, 2005–2015, (2020).
- 15. Noghrehabadi, A., Ghalambaz, M., and Ghanbarzadeh, A., Analysis of second-order velocity slip on forced convection heat transfer in nanofluid flow over a stretching sheet, Powder Technology, 254, 379–386 (2014).

- 16. Rashidi, M. M., et al., Numerical study of convective nanofluid flow over a stretching sheet using spectral relaxation method, Applied Mathematics and Computation, 267, 1006–1016 (2015).
- 17. Haq, R. U., Khan, S. U., and Bhatti, M. M., Numerical simulation of hybrid nanofluid with Joule heating and viscous dissipation, International Communications in Heat and Mass Transfer, 122,105179 (2021).
- 18. Siddiqa, S., Numerical investigation of hybrid nanofluid flow past a stretching surface with slip and heat source/sink effects, Results in Physics, 7, 3071–3081 (2017).
- 19. Khan, M. I., Waqas, M., and Alzahrani, E., Couple stress nanofluid flow with Buongiorno model: A numerical study, Journal of Molecular Liquids, 296,111782 (2019).
- 20. Reddy, G. S., and Chamkha, A. J., Chemical reaction and radiation effects on MHD flow of nanofluids over a stretching sheet, Alexandria Engineering Journal, 54, 755–765, (2015).
- 21. Khan, W. A., and Pop, I., Boundary-layer flow of a nanofluid past a stretching sheet, International Journal of Heat and Mass Transfer, 53, 2477–2483 (2010).

Ummidi Ravi, Madhusudan Patro

Department of Mathematics

Gandhi Institute of Engineering and Technology University, Odisha, 765022, India.

E-mail address: ummidi.ravi@giet.edu, madhusudan@giet.edu

and

Karanam Sreelatha

Department of Mathematics

Satya Institute of Technology and Management, Vizianagaram, A.P., 530041, India.

E-mail address: sreelatha.karanam@sitam.co.in